

Spiking optical patterns and synchronization

Michael Rosenbluh,¹ Yaara Aviad,¹ Elad Cohen,¹ Lev Khaykovich,¹ Wolfgang Kinzel,² Evi Kopelowitz,¹ Pinhas Yoskovits,¹ and Ido Kanter¹

¹*Department of Physics, Bar-Ilan University, Ramat-Gan, 52900 Israel*

²*Institut für Theoretische Physik, Universität Würzburg, Am Hubland 97074 Würzburg, Germany*

(Received 23 April 2007; published 5 October 2007)

We analyze the time resolved spike statistics of a solitary and two mutually interacting chaotic semiconductor lasers whose chaos is characterized by apparently random, short intensity spikes. Repulsion between two successive spikes is observed, resulting in a refractory period, which is largest at laser threshold. For time intervals between spikes greater than the refractory period, the distribution of the intervals follows a Poisson distribution. The spiking pattern is highly periodic over time windows corresponding to the optical length of the external cavity, with a slow change of the spiking pattern as time increases. When zero-lag synchronization between two lasers is established, the statistics of the nearly perfectly matched spikes are not altered. The similarity of these features to those found in complex interacting neural networks, suggests the use of laser systems as simpler physical models for neural networks.

DOI: [10.1103/PhysRevE.76.046207](https://doi.org/10.1103/PhysRevE.76.046207)

PACS number(s): 05.45.Xt, 42.55.Px, 42.65.Sf

Semiconductor lasers, subjected to optical feedback, display chaotic behavior [1]. The chaotic behavior consists of very short and random spiking of the laser intensity with the time interval between spikes depending on how far above lasing threshold the laser is. Two chaotic lasers can be synchronized with each other and this has allowed them to be excellent candidates for novel broadband [2–6] communication devices. Different configurations, such as delayed optoelectronic [7,8] or coherent optical injection [8–11] have been used for synchronization of the two lasers. Using optical feedback, configurations consisting of unidirectional [7,8] or mutual coupling [5,6,8–11] and variations of the strength of the self- and coupling feedback have been shown to result in different synchronization states. The lasers can synchronize in a leader-laggard or anticipated mode, as well as in two different synchronization states; achronal or generalized synchronization [12–14] where the cross correlation of the intensity spikes is time shifted by the feedback delay time but neither laser acts as a preferred leader or laggard or isochronal synchronization (zero-lag) where there is no time delay between the two lasers' chaotic signals [5,6,15–17].

Zero-lag synchronization of lasers was recently extended to a cluster consisting of three semiconductor lasers, mutually coupled along a line, in such a way that the central laser element acts as a relay of the dynamics between the outer elements [18,19]. The zero-lag synchronized dynamics of remotely located chaotic signal sources has sparked an interest in such systems in part because they have features also seen in biological and neural transmission networks. Though the time scales for the two phenomena are vastly different; lasers spiking on 100 ps time scale while neurons spike on ms time scales, much of the dynamics and spiking statistics appear to have common behavior. Here we report on the spiking optical pattern of solitary and two mutually coupled chaotic lasers, observed on a time scale which resolves the individual spikes, in both their synchronized and unsynchronized states and determine the statistical behavior of the spiking. This further allows us to establish an analogy to the spiking behavior of single and interacting neurons.

Our experimental setup is shown schematically in Fig. 1, where two semiconductor lasers are coupled via a partially transmitting mirror placed in the middle of the coupling optical path between the lasers. In the actual experiment the self-feedback and the mutual feedback paths were spatially separated through the use of beam splitters [6]. The time for light propagation from the partially transmitting mirror to one of the lasers is $\tau/2$. We distinguish between the following three limiting scenarios. In the case of a fully reflecting mirror, the lasers are uncoupled and each laser is subject only to a delayed self-feedback. In the second scenario where the mirror is fully transparent, each laser receives a delayed signal from the other, and this configuration is known as “face-to-face.” In the intermediate scenario, the mirror is partially transmitting and each laser is driven by two delayed signals, one from self-coupling and one from mutual coupling.

In the experiment we used Fabry-Perot semiconductor lasers emitting at 670 nm wavelength, selected to have nearly the same threshold current, emission wavelength, and output power. The temperature of each laser is stabilized to better than 0.01 K and the individual laser temperatures are tuned so that the two lasers have nearly identical output wavelengths. The self- and mutual feedback loop time τ is 23.55 ns. Two fast (50 GHz bandwidth) detectors biased via a 40 GHz bandwidth bias T measure the output intensity of each laser. The dc current into the bias T is used to measure the average dc power falling on the detector while the ac currents are measured simultaneously in two channels of a 12 GHz bandwidth, 40 GbGS/s oscilloscope (Tektronix TDS 6124C).

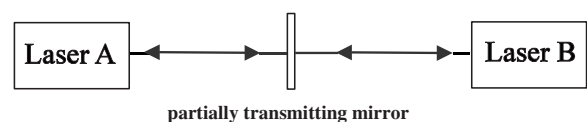


FIG. 1. Schematic experimental setup. Two lasers are mutually coupled via a partially transmitting mirror placed in the middle of the coupling optical path between the lasers.

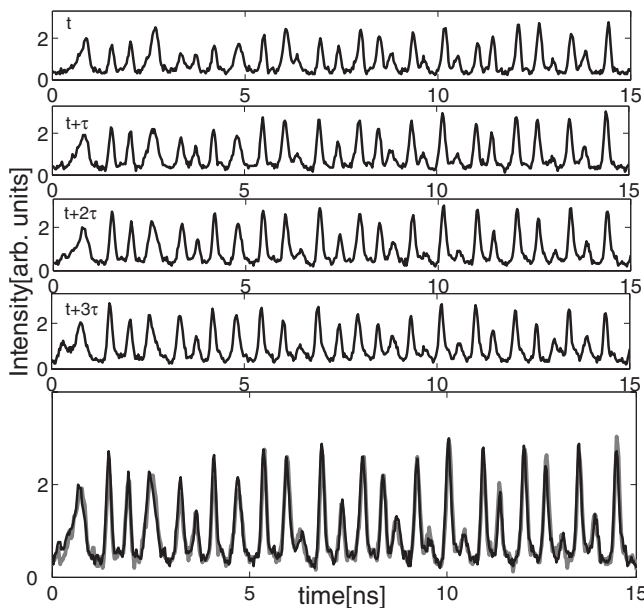


FIG. 2. A trace of 15 ns duration of the intensity of one laser followed by plots of the same laser intensity after a time τ , 2τ , and 3τ with $\tau=23.55$ ns. The laser was operating with $p=1.03$ and with a reflected power of a few % of the laser output intensity. In the bottom panel the intensity trace at time $t+\tau$ and at time $t+2\tau$ are superimposed, demonstrating the slowly decaying periodicity of the spiking pattern.

For the case in which the mirror is fully reflecting the lasers are decoupled. Each laser becomes chaotic due to the self-feedback but the chaotic fluctuations of the lasers are completely independent of each other. A typical trace of one of the laser output intensity measurements as a function of time is presented in the top panel of Fig. 2, for a case when the ratio of the actual laser current to the threshold current p is 1.03. The time dependent intensity of the laser consists of spikes of typical duration of ~ 120 ps. In the following three panels we show the same laser intensity fluctuations recorded after a time, $\tau(=23.55$ ns), 2τ , and 3τ . Figure 2 clearly indicates that on a time scale of a few optical delayed self-feedback times the timing of the spikes repeats itself, where as time elapses the spikes gradually broaden and finally disappear as new spikes emerge in new positions, forming a new pattern. This behavior is physically easy to understand since the feedback photons circulate in the long external cavity with a periodicity τ and the laser receives nearly the same feedback pattern with this periodicity. The photon lifetime in the cavity is finite, however, and thus the feedback waveform slowly changes. After many τ periods (many photon round trips) the feedback waveform and the laser's chaotic fluctuation pattern will have changed completely. From this explanation we can also conclude that the revival of the chaotic pattern with period τ will be nearly independent of p since the chaos is caused and determined by the feedback photon train which has a similar form with period τ . This indeed is also observed in the experiments where the periodicity of the chaotic signal with time τ is independent of p . To further demonstrate the repeatability of the spiking patterns after a delay τ in the bottom panel of

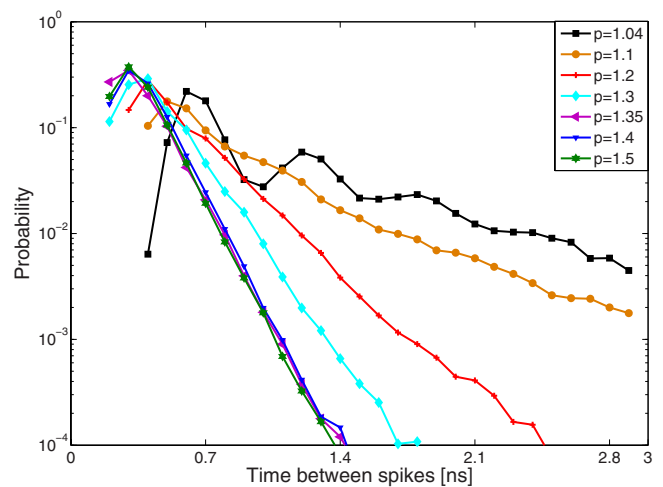


FIG. 3. (Color online) The probability for time intervals between spikes for various values of p .

Fig. 2 we show the overlaid intensity trace at time $t+\tau$ and at time $t+2\tau$.

A quantitative analysis of the spike statistics requires the definition of a low-signal threshold so as to eliminate the small spikes in the measured laser intensity which are the result of noise in the measurements. Our threshold was chosen to be at twice the average detector noise level, and the timing of a spike above this threshold level was determined according to the time of its maximum intensity. For each measurement we accumulated 70 000 consecutive spikes. A histogram of the time interval between consecutive spikes is presented in Fig. 3 for various values of p .

The probability distribution of the time intervals between two spikes consists of two main features. The distribution for relatively long time intervals between the spikes follows a random, Poisson distribution where for small p values the exponential decay rate increases linearly from zero as a function of p , as shown in Fig. 4(a). For very short time intervals the Poisson distribution is altered so that immediately after a spike it is most improbable to record a second spike. The most probable time between consecutive spikes is defined, as for neural spike trains, as the refractory time [20,21]. Figure 4(b) indicates that the refractory time increases as the laser current approaches the threshold value, which makes physical sense, since at low pumping currents it takes longer to rebuild the laser gain after the previous pulse had depleted it.

The chaotic laser dynamics are well described by the three coupled Lang-Kobayashi rate equations for the optical field amplitude E , the optical phase Φ , and the excited carriers n of the gain medium [22]. These equations also predict that the intensity chaos has the form of a spiking behavior of the lasers on a 100 ps time scale, with no laser emission between spikes, in full agreement with the observations. The numerical simulations of the Lang-Kobayashi equations indicate that the reason why after a spike the laser ceases to emit for a refractory time is because the number of carriers drops well below threshold, hence a successive spike is forbidden until the population is repumped again by the laser injection current.

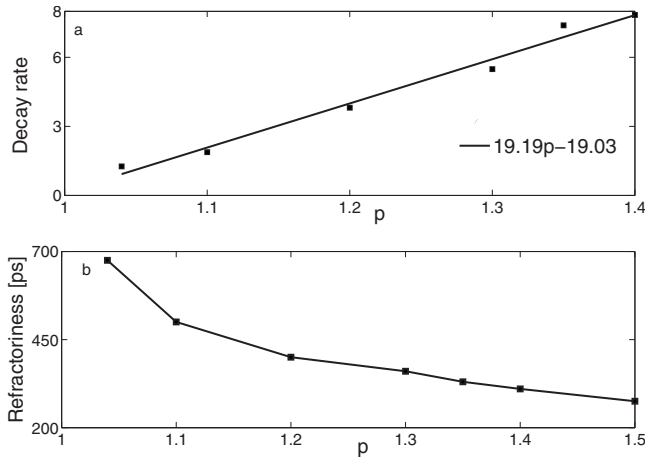


FIG. 4. (a) The exponential decay rate of the probability of time intervals between spikes as a function of p obtained for time intervals greater than the most probable time. The decay rate is a linear function of p for low p values, as indicated by the linear fit (solid line). (b) The most probable time interval, the refractory time, as a function of p .

For the case of a fully transparent mirror, the two face-to-face lasers, operating at nearly identical p values, synchronize achronally. It is convenient to characterize the synchronization via the time dependent cross correlation function for the lasers intensities ρ defined as

$$\rho(\Delta t) = \frac{\sum_i (I_A^i - \langle I_A^{i+\Delta t} \rangle)(I_B^i - \langle I_B^{i+\Delta t} \rangle)}{\sqrt{\sum_i (I_A^i - \langle I_A^{i+\Delta t} \rangle)^2 \sum_i (I_B^i - \langle I_B^{i+\Delta t} \rangle)^2}},$$

where I_A and I_B are the time dependent intensities of lasers A and B . The achronal cross correlation is characterized by two dominant peaks in the intensity cross correlation function at $\pm\tau$. We find that the statistics of the intervals between spikes, the refractory period, and the repetitive spiking pattern with optical delay time τ are not altered. However, when the two face-to-face lasers are configured to have different p values, the lasers no longer synchronize, and from a sample of the signals transmitted between the lasers it is not obvious that one could determine that the two lasers are operating with two different p 's. The statistics of the spike intervals, however, is altered, and reveals not only that the lasers have different p values, but also yields the two p values used in the experiment. To demonstrate this in Fig. 5 we show the distribution of times between spikes when $p_1=1.1$ and $p_2=1.4$ where as previously, the feedback strength for each laser is a few percent of its output power. Figure 5 indicates that the distribution for each of the two lasers is a combination of the distributions of each chaotic solitary laser, as shown in Fig. 3. The distribution consists of two maxima related to the refractoriness connected to p_1 and p_2 . For time intervals greater than both refractory times the distribution follows a Poisson distribution. Similar results are obtained for all combinations of p values lying in the range of 1 to 1.5. Thus a statistical analysis reveals information about, and

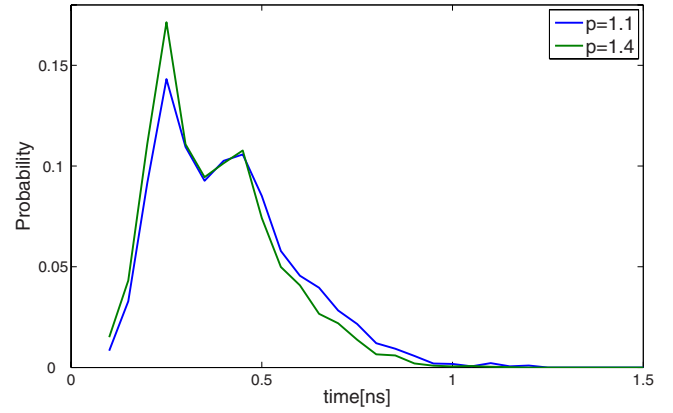


FIG. 5. (Color online) Two lasers in a face-to-face configuration corresponding to a fully transparent mirror in the schematic of Fig. 1. The first laser operates with $p=1.1$ and the second laser with $p=1.4$ and the coupling strength is a few % of the laser intensities. The probability for the time intervals between spikes is presented for each one of the lasers. The two maxima correspond closely to the refractoriness of the solitary lasers operating with $p=1.1$ and 1.4 (see Fig. 3).

differentiates between, two sources operating with different parameters.

Figure 5 indicates that although the two mutually interacting lasers with differing p values are not synchronized, the distribution of the intervals between spikes of each individual laser contains information about the parameter p of the other laser. More precisely, from the measurement of the distribution of spiking time intervals containing the two refractory periods only and using its own known parameter p , each laser can deduce the parameter p of the other laser. This mechanism may play an important role in neurobiology, where the statistical measure of the short intervals among spikes may reveal information about the individual state of the interacting neurons.

For the third scenario of a partially transmitting mirror, each laser receives both self-coupling and mutual coupling signals, and provided that the two lasers have equal or nearly equal p parameters the two lasers synchronize isochronally with zero time lag [15]. The correlation coefficient for the intensity traces averaged over 200 100-ns-long time segments, exceeds 0.95 for $p > 1.2$. The correlation is around 0.9 for p values near 1, where low frequency fluctuations [23] appear which are included in the calculation of the statistics and somewhat degrade the value of the correlation coefficient. In the following we investigate whether the deviation from perfect zero time lag synchronization is caused by a mismatch between the timing of the spikes, by the difference in their heights or by the background noise in our measurements.

Figure 6(a) shows the histogram for the mismatch between the timing of the spikes of the two lasers in the isochronal phase. The histogram indicates that the most probable time difference between the spikes of the two coupled lasers is zero since the average difference between the timing is less than 25 ps, our sampling rate. The width of the histogram, limited by our detection bandwidth, is extremely narrow (< 80 ps), and is not resolved by our detection system.

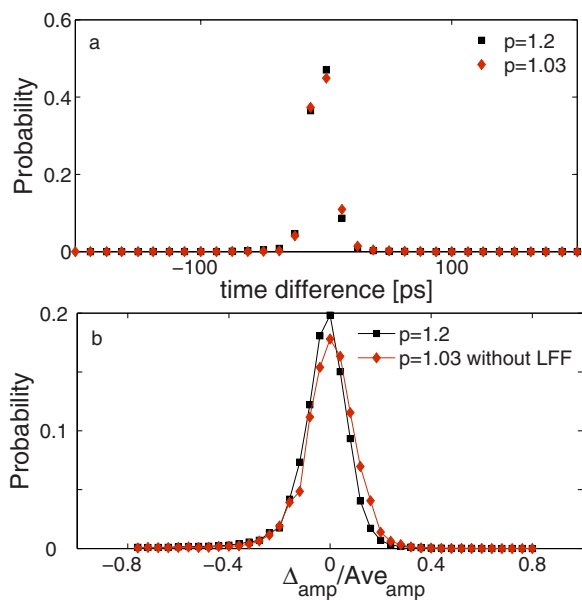


FIG. 6. (Color online) Two lasers in a zero-lag isochronal phase with a partially transmitting mirror in the schematic of Fig. 1. (a) The histogram of the mismatch in the timing of spikes of the two lasers and (b) the relative ratio between the maximum of the intensity of temporally correlated spikes of the two lasers. For the case, $p=1.03$, the probability for the amplitudes was calculated after eliminating the low frequency fluctuations (LFF) from the data.

We also examine the relative difference between the maximum intensities of two correlated spikes in the two lasers, and the histogram consisting of over 60 000 pulses is presented in Fig. 6(b). Shown is the difference between the maximum of each spike for each laser divided by the average of the spike amplitudes Δ_{amp}/ave_{amp} . This result indicates that the average relative difference between the maximum heights of temporally correlated spikes is $\sim 10\%$. It is possible that the mismatch between the maximum intensities of these spikes is much lower, since the maximum intensity measured is very sensitive to the precise sampling time of the oscilloscope relative to the shape of a spike. From these observations we cannot definitively determine the source of the imperfect synchronization, but it appears likely that it is not in the spike timing but rather in the spike amplitude.

Phenomena similar to our observations have been found in the communication of neurons, where immediately after the activation of an action potential it is more difficult to excite a second spike. Neural communication has been documented to have many features (such as refractoriness, the repetitive form of the spiking pattern, synchronization between spatially separated neuron groups, and the spike statistics [19,24,25]) which are similar to those observed for the chaotic lasers. Our demonstration that both the timing and maximum intensities of spikes are extremely well synchronized with zero time lag could have possible important implications for understanding the corresponding phenomena in neural system [26,27]. One of the fundamental questions in neuroscience, for example, is how information is encoded in the neuronal spike trains [28]. Is the information contained in an individual spike form or in the interval between spikes, or is it the mean rate of spikes and timing which matter [29]? Traditionally it has been thought that most of the relevant information was contained in the mean firing rate of the neuron. It is clear, however, that an approach based on a temporal average neglects all the information possibly contained in the exact timing of the spikes and the statistical measure of the short intervals among spikes may reveal information about the individual state of the interacting neurons. Recently more and more experimental evidence has accumulated which suggests that a straightforward firing rate concept based on temporal averaging is too simplistic to describe neural information transfer. If, at each processing step, neurons had to wait and perform a temporal average in order to read the message, the reaction time would be incompatibly long compared to experimental evidence.

In conclusion, our results for chaotic lasers show that individual spiking laser units are able to generate irregular spike patterns which become synchronized when two such units are coupled to each other, without any time delay, although the transmission time can be relatively long. Synchronization is maintained even on the time scale of individual spike widths. For chaotic lasers, transmission of information by the spiking pattern has been demonstrated, and the repetitive bar-code pattern we observe has features which are useful for communication applications of these signals. The similarity of the lasers to neural systems is noted, and it is possible that complex neural systems can be effectively modeled by the much simpler and much more flexible and well-controlled experimental environment of coupled laser systems.

- [1] H. Schuster and W. Just, *Deterministic Chaos* (Wiley VCH, New York, 2005).
- [2] P. Colet and R. Roy, *Opt. Lett.* **19**, 2056 (1994).
- [3] G. D. VanWiggeren and R. Roy, *Science* **279**, 1198 (1998).
- [4] A. Argyris, D. Syvridis, L. Larger, V. Annovazzi-Lodi, P. Colet, I. Fischer, J. Garcia-Ojalvo, C. R. Mirasso, L. Pesquera, and K. A. Shore, *Nature (London)* **438**, 343 (2005).
- [5] E. Klein, R. Mislavaty, I. Kanter, and W. Kinzel, *Phys. Rev. E*

- 72**, 016214 (2005).
- [6] E. Klein, N. Gross, E. Kopelowitz, M. Rosenbluh, L. Khaykovich, W. Kinzel, and I. Kanter, *Phys. Rev. E* **74**, 046201 (2006).
- [7] Jia-Ming Liu, How-Foo Chen, and Shou Tang, *IEEE J. Quantum Electron.* **38**, 1184 (2002).
- [8] S. Tang and J. M. Liu, *IEEE J. Quantum Electron.* **39**, 708 (2003).

- [9] T. Heil, I. Fischer, W. Elsasser, J. Mulet, and C. Mirasso, *Phys. Rev. Lett.* **86**, 795 (2001).
- [10] A. Hohl, A. Gavrielides, T. Erneux, and V. Kovanis, *Phys. Rev. A* **59**, 3941 (1999).
- [11] S. Sivaprakasam, E. M. Shahverdiev, P. S. Spencer, and K. A. Shore, *Phys. Rev. Lett.* **87**, 154101 (2001).
- [12] A. Murakami and J. Ohtsubo, *Phys. Rev. A* **65**, 033826 (2002).
- [13] R. Vicente, T. Perez, and C. R. Mirasso, *IEEE J. Quantum Electron.* **38**, 1197 (2002).
- [14] H. Erzgraber, D. Lenstra, B. Krauskopf, E. Wille, M. Peil, I. Fischer, and W. Elsasser, *Opt. Commun.* **255**, 286 (2005).
- [15] E. Klein, N. Gross, M. Rosenbluh, W. Kinzel, L. Khaykovich, and I. Kanter, *Phys. Rev. E* **73**, 066214 (2006).
- [16] I. Kanter, N. Gross, E. Klein, E. Kopelowitz, P. Yoskovits, L. Khaykovich, W. Kinzel, and M. Rosenbluh, *Phys. Rev. Lett.* **98**, 154101 (2007).
- [17] N. Gross, W. Kinzel, I. Kanter, M. Rosenbluh, and L. Khaykovich, *Opt. Commun.* **267**, 464 (2006).
- [18] I. Fischer, R. Vicente, J. M. Buldu, M. Peil, C. R. Mirasso, M. C. Torrent, and J. Garcia-Ojalvo, *Phys. Rev. Lett.* **97**, 123902 (2006).
- [19] A. Cho, *Science* **314**, 37 (2006).
- [20] M. J. Berry and M. Meister, *J. Neurosci.* **18**, 2200 (1998).
- [21] F. Rieke, D. Warland, R. de Ruyter van Steveninck, and W. Bialek, *Spikes—Exploring the Neural Code* (MIT Press, Cambridge, MA, 1996).
- [22] R. Lang and K. Kobayashi, *IEEE J. Quantum Electron.* **QE-16**, 347 (1980).
- [23] V. Ahlers, U. Parlitz, and W. Lauterborn, *Phys. Rev. E* **58**, 7208 (1998).
- [24] A. K. Engel, P. Koenig, A. K. Kreiter, and W. Singer, *Science* **252**, 1177 (1991).
- [25] P. R. Roelfsema, A. K. Engel, P. Koenig, and W. Singer, *Nature (London)* **385**, 157 (1997).
- [26] W. Gerstner and W. Kistler, *Spiking Neuron Models* (Cambridge University Press, Cambridge, 2002).
- [27] M. Abeles, in *Models of Neural Networks II* (Springer-Verlag, New York, 1994).
- [28] B. W. Connors and M. J. Gutnick, *Trends Neurosci.* **13**, 99 (1990).
- [29] P. R. Gray, *Biophys. J.* **7**, 759 (1967).